



Topological Structure Optimization and Kinematic Performance Improvement of 3-RRR Planar Parallel Manipulator*

Ke XU¹, Huiping SHEN^{*2}, Jiaming DENG³, Yunyu SHEN⁴

¹ School of Mechanical Engineering, Changzhou University
Chang Zhou 213016 China

1375928645@qq.com

² * shp65@126.com

³ czdydjm@126.com

⁴ Business Administration Department, University of Northeastern
Shen Yang 110819 China
919304858@qq.com

Abstract

The typical 3-RRR planar parallel manipulator with two translations and one rotation has extensive applications such as plane location and motion transfer. But it suffers two disadvantages. One is its analytical direct kinematics is difficult to be got and another is not input-output motion decoupled. This paper focuses on its topological structure optimization and resulting kinematic performance improvement. First, the coupling degree of this manipulator is calculated being $k=1$. Second, based on structure coupling-reducing principle, its coupling-reduced manipulator with zero coupling degree is designed, which not only leads to be easy to get its analytic direct kinematic solutions, but also makes input-output motion partially decoupled. Moreover, based on workspace and singularity of this coupling-reduced manipulator, comprehensive comparison of two manipulators before and after coupling-reducing showed that the main performances of structure coupling-reduced manipulator are superior than that of the typical mechanism. The work shows that structure coupling-reducing is effective method for optimization of topology structure.

Keywords: Parallel mechanism, Direct kinematics, Structure coupling-reducing, Performance analysis.

1. Introduction

3-RRR planar parallel manipulator has potential value in practical application. It not only can be used in guiding, location and transmission of rigid body, but also can obtain

more accurate motion trajectory than general multi-bar linkages do [1].

At present, many scholars have had much more investigation for 3-RRR planar parallel manipulator. In the aspect of the direct kinematics, the number of the maximum direct kinematics of 3-RRR manipulator is 6, which is proved by [2]. Oetomo *et.al* [3] set up three constraint equations and then got one eighth degree polynomial to solution by using the elimination method.

In the way of mechanism's performance investigation, Gosselin[4] conducted the optimization parameter design of 3-RRR manipulator. Wu *et.al* [5] made comparisons on the peculiarities of statics and dynamics between 4-RRR, 3-RRR and 2-RRR. Taking prismatic pair as actuated one, Cha *et.al* [6] measured the range of 3-RRR manipulator's nonsingular paths. Wei *et.al* [7] analyzed 8 kinds topology structure of 3-RRR manipulator, and analyzed this manipulator dexterity by taking conditioning performance of Jacobian matrix as index. The reachable workspace of the symmetric 3-RRR parallel manipulator was analyzed by Li *et.al* [8]. The Dexterous workspace of 3-RRR manipulator was obtained in [9, 10]. Gao *et. al* [11] systematically analyzed the relationship between branched chains' length and the workspace shape of 3-RRR manipulator.

Obviously, current studies on 3-RRR manipulator focus primarily on workspace, singularity, dexterity and stiffness performance. However, accuracy analysis and design of the manipulator are difficult and motion control is comparatively complex, the reasons of which are that the analytical solutions for this manipulator are not easy to

get its direct kinematics, and further the manipulator does not possess input-output (I-O) motion decoupling.

Taking the two reasons stated above as target, this paper design firstly a novel kind of coupling-reduced mechanism(CRM) with low coupling degree, i.e., $k=0$, and motion-decoupling based on the structure coupling-reducing methodology. Not only are analytical solutions for direct kinematics obtained but also this manipulator has I-O decoupling, which accordingly leads to the precision design, motion planning and control of this manipulator be easy. Moreover, the workspace and singularity are analyzed. The work shows that the comprehensive performance of CRM is better than the typical manipulator 3-RRR. Therefore typical 3-RRR planar parallel manipulator could be replaced by the CRM.

2. 3-RRR PM and Its Topological Optimization Design

Typical 3-RRR planar manipulator is shown in Fig. 1. The digitals, from 1 to 7, are denoted as different rods. The moving platform 1, an equilateral triangle, connects with the static platform 0 through three RRR branch chains. The static coordinate system o - xy and the moving coordinate system o' - $x'y'$ are established on the static platform 0, moving platform 1 respectively.

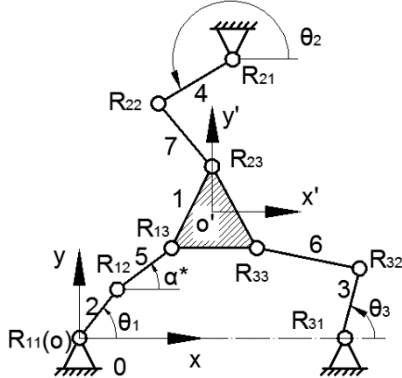


Fig. 1. 3-RRR planar parallel mechanism

Length for each link of three branch chains are given as follows, respectively.

$$R_{11}R_{12}=l_1, R_{12}R_{13}=l_2, R_{21}R_{22}=l_7, \\ R_{22}R_{23}=l_6, R_{31}R_{32}=l_5, R_{32}R_{33}=l_4.$$

The side length of moving platform 1 is l_3 , its attitude angle γ is anticlockwise direction of x axis to x' , The input angle of three actuated pairs, R_{11} , R_{21} , R_{31} , is θ_1 , θ_2 , θ_3 respectively, as shown in the Fig.1.

A. Coupling Degree (κ) of 3-RRR Manipulator

According to the structure composition theory of parallel mechanisms based on the ordered single-open-chain (SOC) [12], this mechanism can be decomposed into

following two SOC. The restraint degree (Δ) of each SOC is listed as follows, respectively.

$$SOC_1 \{-R_{11}-R_{12}-R_{13}-R_{32}-R_{31}-\}$$

$$\Delta_1 = \sum_{i=1}^6 f_i - I_1 - \xi_{L_1} = 6 - 2 - 3 = 1$$

$$SOC_2 \{-R_{21}-R_{22}-R_{23}-\}$$

$$\Delta_2 = \sum_{i=1}^3 f_i - I_2 - \xi_{L_2} = 3 - 1 - 3 = -1$$

k of the manipulator is calculated by

$$k = \frac{1}{2} \sum_{j=1}^2 |\Delta_j| = \frac{1}{2} (|1| + |-1|) = 1$$

Here,

I_j - the number of inputs in the j^{th} SOC,

f_i - DOF of the i^{th} kinematic pairs,

ξ_{L_j} - the number of independent equations of j^{th} ,

Δ_j -constraint degree of j^{th} SOC.

Since the coupling degree of this manipulator is $k=1$, its numerical solutions of direct kinematics could be obtained by solving a one-variable polynomial equation. That is, one virtual variable is needed to be assigned to SOC₁ so that direct kinematic equation containing the variable can be established easily. Then one-dimensional search method is utilized easily to obtain its numerical direct solutions for this manipulator. The calculation is complicated and time-consuming, which is not benefit for real-time controlling. It does not good for the accuracy design of this manipulator as well.

At the same time, since every output parameter (x , y , γ) of moving platform 1 is related to all of three input angles θ_1 , θ_2 , and θ_3 , the manipulator does not possess I-O motion decoupling, which is also undesirable for path planning and motion controlling.

B. Topological Optimization Design of the Structure

In order to improve the two disadvantages stated above, we implement an optimization design for topological structure of this manipulator. Based on the coupling-reducing principle of mechanism topology [13], we combine two arbitrary pairs on the movable platform, such as R_{13} and R_{33} in the Fig. 1, into one multiple joint, and other conditions are not changed, which lead to a modified manipulator shown in the Fig. 2.

For the modified manipulator, moving platform 1 has degenerated from three-joint rod to two-joint rod, i.e., R_3R_{23} . Its topological analysis can be decomposed into following:

$$SOC_1 \{-R_{11}-R_{12}-R_3-R_{32}-R_{31}-\}$$

$$\Delta_1 = \sum_{i=1}^5 f_i - I_1 - \xi_{L_1} = 5 - 2 - 3 = 0$$

$$SOC_2 \{-R_{21}-R_{22}-R_{23}-R_3-\}$$

$$\Delta_2 = \sum_{i=1}^3 f_i - I_2 - \xi_{L_2} = 4 - 1 - 3 = 0$$

Therefore, $k = \frac{1}{2} \sum_{j=1}^2 |\Delta_j| = \frac{1}{2} (|0| + |0|) = 0$

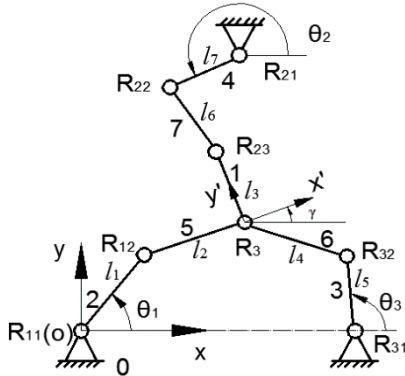


Fig 2. 3-dof coupling-reducing mechanism (CRM)

It means that the coupling degree of this modified manipulator is reduced from one to zero, and its analytic expression of direct kinematics can be directly and conveniently obtained. Meanwhile, the modified manipulator is now already I-O motion decoupled. The concrete analysis is as follows. We called the modified manipulator as coupling-reducing mechanism (CRM).

3. Kinematic Analysis of CRM

A. Direct Kinematics

The problem of the direct kinematics can be described as: with three known input angles θ_1 , θ_2 , and θ_3 , it is required to solve the attitude angle γ and position (x, y) of revolute joint R_3 of the moving platform 1.

The static coordinate system $o-xy$ is shown in Fig. 2, which is the same with it in Fig. 1. The moving coordinate system $R_3-x'y'$ are established on R_3 , y' axis that coincides with the line R_3R_{23} . x' axis is perpendicular to this line. The attitude angle γ of the moving platform 1 is taken from forward direction of x' axis to x as well. The coordinates R_{11} , R_{21} , R_{31} are not changed such that $(0,0)$, (l_9, l_{10}) , $(l_8, 0)$, respectively. When input angles θ_1 , θ_2 and θ_3 are given, the coordinates of joints R_{12} , R_{22} , and R_{32} are easily got.

- Solve the coordinates of R_3 by using the positions of R_{12} , R_{32}

Based on $R_{12}R_3=l_2$, $R_{32}R_3=l_4$,

$$\begin{cases} (x_{R_3} - x_{R_{12}})^2 + (y_{R_3} - y_{R_{12}})^2 = l_2^2 \\ (x_{R_3} - x_{R_{32}})^2 + (y_{R_3} - y_{R_{32}})^2 = l_4^2 \end{cases}$$

It is obtained

$$\begin{cases} x_{R_3} = \frac{-E \pm \sqrt{E^2 - 4DF}}{2D} \\ y_{R_3} = \frac{C}{B} - \frac{A}{B} x_{R_3} \end{cases} \quad (1)$$

where

$$\begin{aligned} A &= 2(l_1 \cos \theta_1 - l_8 - l_5 \cos \theta_3), \\ B &= 2(l_1 \sin \theta_1 - l_5 \sin \theta_3), \\ C &= l_4^2 - l_2^2 + l_1^2 - l_8^2 - l_5^2 - 2l_5 l_8 \cos \theta_3, \\ D &= A^2 + B^2, \\ E &= 2l_1 A B \sin \theta_1 - 2l_1 B^2 \cos \theta_1 - 2AC, \\ F &= C^2 + l_1^2 B^2 - 2l_1 B C \sin \theta_1 - l_2^2 B^2. \end{aligned}$$

- Solve the coordinate of R_{23} by using the positions of R_{22} , R_3

Based on $R_{23}R_3=l_3$, $R_{22}R_{23}=l_6$

$$\begin{cases} (x_{R_3} - x_{R_{23}})^2 + (y_{R_3} - y_{R_{23}})^2 = l_3^2 \\ (x_{R_{23}} - x_{R_{22}})^2 + (y_{R_{23}} - y_{R_{22}})^2 = l_6^2 \end{cases}$$

We have

$$\begin{cases} x_{R_{23}} = \frac{-e \pm \sqrt{e^2 - 4df}}{2d} \\ y_{R_{23}} = \frac{c}{b} - \frac{a}{b} x_{R_{23}} \end{cases} \quad (2)$$

Here,

$$\begin{aligned} a &= 2(x_{R_3} - l_9 - l_7 \cos \theta_2), \\ b &= 2(y_{R_3} - l_{10} - l_7 \sin \theta_2), \\ c &= l_6^2 - l_3^2 + x_{R_3}^2 + y_{R_3}^2 - l_9^2 - l_7^2 - l_{10}^2 \\ &\quad - 2l_{10} l_7 \sin \theta_2 - 2l_9 l_7 \cos \theta_2, \\ d &= a^2 + b^2, \\ e &= 2y_{R_3} ab - 2x_{R_3} b^2 - 2ac, \\ f &= c^2 + (x_{R_3}^2 + y_{R_3}^2 - l_3^2) b^2 - 2y_{R_3} bc. \end{aligned}$$

Then, attitude angle γ is expressed as

$$\tan \gamma = (y_{R_{23}} - y_{R_3}) / (x_{R_{23}} - x_{R_3}) \quad (3)$$

According to Eq.(1), the position of the moving platform 1, i.e., (x_{R_3}, y_{R_3}) , is confirmed by two input angles θ_1 , θ_3 . It is also known from Eq. (3) that attitude angle γ is confirmed by three input angles θ_1 , θ_2 , and θ_3 . Therefore, the CRM possess I-O partial motion decoupling property. Consequently, it is easier to conduct path planning and motion control of the CRM compared with the typical manipulator.

B. Inverse Kinematics

The problem of the inverse kinematics analysis is described as for given attitude angle γ and position (x, y) of

joint R_3 of moving platform 1, it is required to solve three input angles $\theta_1, \theta_2, \theta_3$.

In the moving coordinate system $R_3-x'y'$, the coordinate of R'_{23} is $(0, l_3)$. Through the coordinate system conversion between the static and moving coordinate one, the coordinate of R_3 is

$$\begin{bmatrix} x_{R_{23}} \\ y_{R_{23}} \end{bmatrix} = \begin{bmatrix} \cos \gamma & -\sin \gamma \\ \sin \gamma & \cos \gamma \end{bmatrix} \begin{bmatrix} 0 \\ l_3 \end{bmatrix} + \begin{bmatrix} x \\ y \end{bmatrix} = \begin{bmatrix} -l_3 \sin \gamma + x \\ l_3 \cos \gamma + y \end{bmatrix}$$

Based on $R_{12}R_3=l_2$, $R_{32}R_3=l_4$, $R_{22}R_{23}=l_6$, three constraint equations can be expressed as

$$(x_{R_{12}} - x_{R_3})^2 + (y_{R_{12}} - y_{R_3})^2 = l_2^2 \quad (4)$$

$$(x_{R_{22}} - x_{R_{23}})^2 + (y_{R_{22}} - y_{R_{23}})^2 = l_6^2 \quad (5)$$

$$(x_{R_{32}} - x_{R_3})^2 + (y_{R_{32}} - y_{R_3})^2 = l_4^2 \quad (6)$$

According to Eqs.(4)~(6), the inverse kinematic for the CRM can be expressed as

$$\theta_i = 2 \arctan \frac{A_i \pm \sqrt{A_i^2 + B_i^2 - C_i^2}}{B_i - C_i}, \quad i=1, 2, 3 \quad (7)$$

Here,

$$A_1 = 2y_{R_3}l_1; \quad B_1 = 2x_{R_3}l_1,$$

$$C_1 = l_2^2 - l_1^2 - x_{R_3}^2 - y_{R_3}^2,$$

$$A_2 = 2y_{R_{23}}l_7 - 2l_{10}l_7,$$

$$B_2 = 2x_{R_{23}}l_7 - 2l_9l_7,$$

$$C_2 = l_6^2 + 2x_{R_{23}}l_9 + 2y_{R_{23}}l_{10} - l_7^2 - l_9^2 - l_{10}^2 - x_{R_{23}}^2 - y_{R_{23}}^2,$$

$$A_3 = 2y_{R_3}l_5; \quad B_3 = 2x_{R_3}l_5 - 2l_8l_5,$$

$$C_3 = l_4^2 + 2x_{R_3}l_8 - l_5^2 - l_8^2 - x_{R_3}^2 - y_{R_3}^2.$$

C. Numerical Examples

As shown in Fig. 2, the structural parameters, based on Ref.[4], of the CRM are shown as follows.

$$l_1 = l_5 = l_7 = 400, \quad l_8 = 600, \quad l_2 = l_3 = l_4 = l_6 = 300, \\ l_9 = 1054.1, \quad l_{10} = 1045.4 \text{ (units: mm)}.$$

Three input angles θ_1, θ_2 , and θ_3 are $60^\circ, 240^\circ, 70^\circ$, respectively. The substitution of the known parameters into Eqs.(1)~(3) gives two sets direct kinematics solutions shown in Tab 1.

Tab 1. Direct kinematics of the CRM

| | x | y | γ |
|----|-------|-------|------------|
| I | 461.1 | 494.1 | -104.8544° |
| II | 461.1 | 494.1 | -20.0847° |

It is easy to verify the correctness of these direct kinematics solutions by using the inverse kinematic Eq. (7). It is omitted for the limited space.

D. Workspace Analysis

• Reachable workspace

Reachable workspace is reachable area of a moving platform. It is one of main performance indexes to evaluate the kinematic performances of manipulator [8].

The CRM is derived from 3-RRR manipulator by combining two revolute joints R_{13} and R_{33} , and length of other links does not change at all. According to the structural parameters of [10], lengths of the CRM are as follows.

$$l_1 = l_5 = l_7 = 200, \quad l_2 = l_4 = l_6 = 200, \quad l_3 = 100\sqrt{3}, \\ l_8 = 300, \quad l_9 = 150, \quad l_{10} = 150\sqrt{3} \text{ (units: mm)}.$$

Through programming computation on MATLAB, the reachable workspace acreage of 3-RRR typical manipulator is $3.5868 \times 10^7 \text{ mm}^2$, and its shape is shown in Fig.3 (a). The reachable workspace area of the CRM is $2.6095 \times 10^7 \text{ mm}^2$, and its shape is shown in Fig.3 (b).

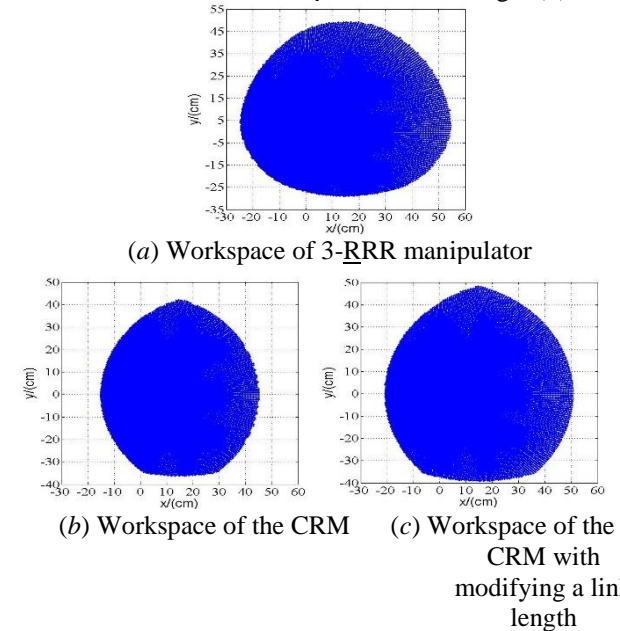


Fig 3. Reachable Workspace comparison between the CRM and typical mechanism

It is easy from the Fig.3 to find that the area of the CRM is 27.25% less than typical manipulator. However, reachable workspace of the CRM can be improved and became larger by means of increasing some link lengths. For instance, when length of the links 2,3,4,5,6, and 7 are increased to one-sixth of the length of link 1, i.e., $l_3/6$, the area of the CRM will be $3.7948 \times 10^7 \text{ mm}^2$, for which the incremental of about 5.52% is made more than that of the typical manipulator. Moreover, the shape has symmetry and succession as well, as shown in Fig.3(c).

• Dexterous workspace

If the attitude angle can change arbitrarily in the range of 0° to 360° when the moving platform moves, the motion area of base point is called as dexterous workspace [9, 10].

For the 3-RRR typical manipulator shown in Fig.1, the center of the moving platform 1 is taken as the base point O' . If the base point O' in the range of dexterous workspace, the moving platform 1 can rotate completely around this base point.

We assume that the moving platform 1 is connected with the frame at the point O' using the revolute joint $R_{O'}$, and only one constraint chain i , for example, $i=1$, is considered, one fictitious and subsidiary four-bar linkage $R_{i1}R_{i2}R_{i3}R_{O'}$ is obtained. The length L of the frame will change along with the position change of the base point O' . But the crank $R_{i3}R_{O'}$ can move completely around the joint $R_{O'}$. The structural parameters of this subsidiary four-bar linkage are given as follows.

$$R_{i1}R_{i2}=L_1, R_{i2}R_{i3}=L_2, R_{i3}R_{O'}=L_3, R_{i1}R_{O'}=L.$$

Based on the crank existence conditions of the four-bar linkage, the range of length L can be taken as

$$L = (0, r_1] \cup [r_2, r_3] \quad (8)$$

where $r_1 = L_3 - (L_1 - L_2)$, $r_2 = (L_1 - L_2) + L_3$, $r_3 = (L_1 + L_2) - L_3$.

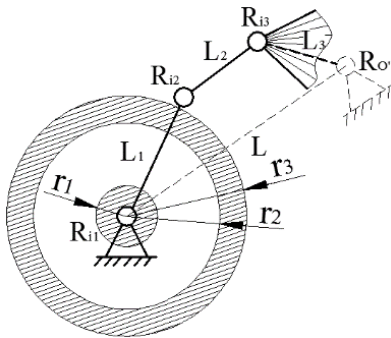


Fig. 4. Dexterous workspace in the constraint of branded chain i

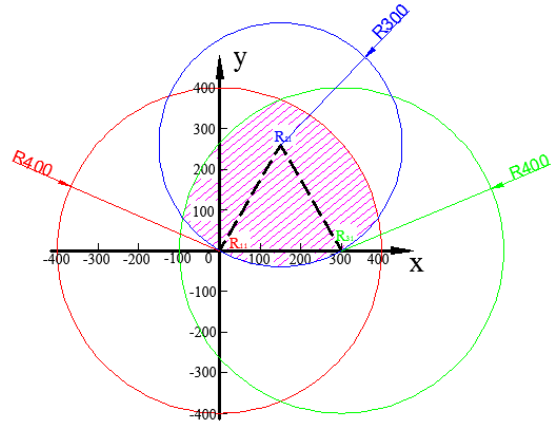
If taking R_{i1} as center of a circle and r_1, r_2, r_3 as radius, three circles can be drawn respectively. Then, the base point O' locates inside the circle area of between radius r_2 and r_3 or the circle with a radius of r_1 , i.e., the shadow area shown in Fig.4, which is denoted by I_i .

When we consider the combined action of three chains I_1, I_2 and I_3 , dexterous workspace W is the intersection workspace that chains I_1, I_2 and I_3 produce together.

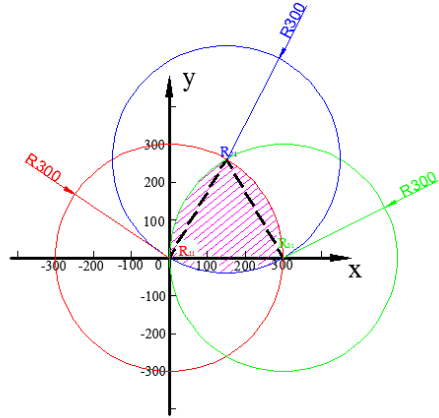
For the CRM and its chain 1 and 3, we assign $r_1=r_2=0$, $r_3=400$, and we assign $r_1=r_2=0$, $r_3=300$ for the chain 2.

For 3-RRR manipulator and its three chains, we assign $r_1=r_2=0$, $r_3=300$. Therefore, the dexterous workspaces of the CRM and 3-RRR manipulator are calculated and shown in Fig.5(a) and Fig.5(b) respectively.

We find that the dexterous workspace area of the CRM and typical mechanism are $8.6567 \times 10^6 \text{ mm}^2$, $6.3429 \times 10^6 \text{ mm}^2$, respectively, and the former is 36.48% bigger than the later.



(a) Dexterous workspace of the CRM



(b) Dexterous workspace of the 3-RRR typical manipulator

Fig. 5. Dexterous workspace comparison between the CRM and typical manipulator

E. Singularity Analysis

• Singularity analysis method

If vectors representing all input motions and output motions are denoted by X and Y respectively, the relationship between X and Y can be expressed as following [14].

$$F(X, Y) = 0 \quad (9)$$

By simplifying and rearranging equation (9), then taking the time derivative of the two sides of the resulting equation, the following equation is obtained.

$$J_p \dot{X} - J_q \dot{Y} = 0 \quad (10)$$

Based on whether J_p and J_q matrix are singular, the singular posture of the mechanism could be classified three types as follows

1. When $\det(J_q) = 0$, input singularity happens.
2. When $\det(J_p) = 0$, output singularity happens.
3. When $\det(J_q) = \det(J_p) = 0$, hybrid singularity happens.

- Calculate of \mathbf{J}_p and \mathbf{J}_q matrix

By taking the time derivative of the two sides of Eqs. (4)~(6), the following equation is obtained.

$$u_{ii}\dot{\theta}_i - f_{i1}\dot{x} - f_{i2}\dot{y} - f_{i3}\dot{z} = 0, i=1,2,3. \quad (11)$$

Hence, $\mathbf{v} = [\dot{x} \ \dot{y} \ \dot{z}]^T$ is the output speed of the end effector of the mechanism, while $\boldsymbol{\omega} = [\dot{\theta}_1 \ \dot{\theta}_2 \ \dot{\theta}_3]^T$ is actuated joint input angle velocity. The relationship between \mathbf{V} and $\boldsymbol{\omega}$ is as:

$$\mathbf{J}_p \mathbf{V} = \mathbf{J}_q \boldsymbol{\omega} \quad (12)$$

Where,

$$\mathbf{J}_p = \begin{bmatrix} f_{11} & f_{12} & f_{13} \\ f_{21} & f_{22} & f_{23} \\ f_{31} & f_{32} & f_{33} \end{bmatrix}; \quad \mathbf{J}_q = \begin{bmatrix} u_{11} & & \\ & u_{22} & \\ & & u_{33} \end{bmatrix};$$

$$u_{11} = l_1(y_{R_{12}} - y_{R_3})\cos\theta_1 - l_1(x_{R_{12}} - x_{R_3})\sin\theta_1,$$

$$u_{22} = l_7(y_{R_{22}} - y_{R_{23}})\cos\theta_2 - l_1(x_{R_{22}} - x_{R_{23}})\sin\theta_2,$$

$$u_{33} = l_5(y_{R_{32}} - y_{R_3})\cos\theta_3 - l_5(x_{R_{32}} - x_{R_3})\sin\theta_3,$$

$$f_{11} = x_{R_{12}} - x_{R_3}, f_{12} = y_{R_{12}} - y_{R_3}, f_{13} = 0,$$

$$f_{21} = x_{R_{22}} - x_{R_{23}}, f_{22} = y_{R_{22}} - y_{R_{23}},$$

$$f_{23} = l_3(x_{R_{23}} - x_{R_{22}})\cos\gamma + l_3(y_{R_{23}} - y_{R_{22}})\sin\gamma,$$

$$f_{31} = x_{R_{32}} - x_{R_3}, f_{32} = y_{R_{32}} - y_{R_3}, f_{33} = 0.$$

- Singularity comparison between the CRM and 3-RRR typical mechanism

(1) Input singularity

When the input singularity happens, the movable platform 1 of this mechanism will lose its motion ability along some directions. This moment, at least one motion chain reaches at the boundary of workspace, and we have

$$\det(\mathbf{J}_q) = 0$$

The solution set \mathbf{A} of this equation is shown below

$$\mathbf{A} = \{\mathbf{A}_1 \cup \mathbf{A}_2 \cup \mathbf{A}_3\} \quad (13)$$

Here

$$\mathbf{A}_1 = \{(y_{R_{12}} - y_{R_3})\cos\theta_1 - (x_{R_{12}} - x_{R_3})\sin\theta_1 = 0\}, \text{ which}$$

means that three points R_{11} , R_{12} and R_3 are collinear.

$$\mathbf{A}_2 = \{(y_{R_{22}} - y_{R_{23}})\cos\theta_2 - (x_{R_{22}} - x_{R_{23}})\sin\theta_2 = 0\},$$

which means that three points R_{23} , R_{22} and R_{21} are collinear.

$$\mathbf{A}_3 = \{(y_{R_{32}} - y_{R_3})\cos\theta_3 - (x_{R_{32}} - x_{R_3})\sin\theta_3 = 0\}, \text{ which}$$

means that three points R_{31} , R_{32} and R_3 are collinear.

When three points R_{11} , R_{12} and R_3 are collinear, link 2 and link 5 have combined into one line 2-5. Then, an imaginary four-bar linkage is denoted by link 0, 2-5, 6 and 3, $\theta_3 = f(\theta_1)$, and θ_2 is also independent input angle. The path of joint R_3 on the moving platform 1 is the part arc with a radius of line 2-5. The length of this arc is determined by the two chains 2 and 3.

However, for the 3-RRR typical manipulator when three points R_{11} , R_{12} and R_{13} are collinear, three input angles are independent each other. Moreover, the motion of moving platform 1 is not restrictive when the joint R_{13} is fixed (Fig.1). The base point O' locates inside the circular ring that is determined by the circular radius $l_{2-5} + R_{13}O'$ and $l_{2-5} - R_{13}O'$, the upper and lower boundary of this part annulus are determined by the motion limitation of other two branched chains.

Because of the symmetry, singularity analysis for the case \mathbf{A}_2 and \mathbf{A}_3 is similar with that of the above stated.

(2) Output singularity

Under this circumstance, the movable platform 1 still has local motion when all actuated joints are locked. If the movable platform 1 is applied by a limited force, three input links need infinite actuated force to achieve force balance. By this time, we have $\det(\mathbf{J}_p) = 0$, the solution of the set \mathbf{B} for this equation is shown below

$$\mathbf{B} = \{\mathbf{B}_1 \cup \mathbf{B}_2\} \quad (14)$$

Here,

$$\mathbf{B}_1 = \{(x_{R_{23}} - x_{R_{22}})\cos\gamma + (y_{R_{23}} - y_{R_{22}})\sin\gamma = 0\}, \text{ which means}$$

that three points R_{22} , R_{23} and R_3 are collinear.

$$\mathbf{B}_2 = \{f_{12}f_{31} - f_{11}f_{32} = 0\}, \text{ which means that three}$$

points R_{12} , R_{32} and R_3 are collinear.

Three kinds of the output singular configurations of the CRM are shown in Eq.(14). When the formula \mathbf{B}_1 is satisfied three points R_{22} , R_{23} and R_3 are collinear. When taking θ_1 , θ_3 as the independent input angles, the angle θ_2 , i.e., $\theta_2 = f(\theta_1, \theta_3)$, is a dependent input.

However, for 3-RRR typical mechanism, it exists four kinds of singular configurations as follows

1. Four joints R_{12} , R_{13} , R_{33} and R_{32} are collinear.
2. Four points R_{12} , R_{13} , R_{23} and R_{22} are collinear.
3. Four points R_{22} , R_{23} , R_{33} and R_{32} are collinear.
4. Links 5, 6 and 7 intersect at one point outside the moving platform.

For example, when the first kind of singularity of 3-RRR mechanism happens, i.e., case ①, input θ_1 , θ_2 are taken as the independent ones, the angle θ_3 is dependent input such as $\theta_3 = f(\theta_1)$.

(3) Synthesis singularity

When $\det(\mathbf{J}_q) = \det(\mathbf{J}_p) = 0$ is satisfied, the input and output singularity will happen at the same time. For instance, if the equations \mathbf{A}_1 and \mathbf{B}_1 are satisfied, three points R_{11} , R_{12} and R_3 , and another three points R_{22} , R_{23} and R_3 are collinear respectively.

It is clear that from the discussion above, the hybrid singularity analysis of the CRM is simpler than 3-RRR typical manipulator. This conclusion is obtained respectively by a comprehensive comparison of the input and output singularity of the two mechanisms.



4. Performance Comparison

In a word, the performance comparison of these two mechanisms is shown in Tab 2.

Table 2. Performance comparison of the CRM and 3-RRR typical manipulator

| Performance | CRM | 3-RRR |
|----------------------|-------------------|-----------|
| k | 0 | 1 |
| Direct kinematics | Analytic | Numerical |
| I - O decoupling | Yes | No |
| Reachable workspace | Slightly smaller* | Bigger |
| Dexterous workspace | Big | Small |
| Singularity | Simple | Complex |

*Note: The size of reachable workspace of CRM could be improved or increased by magnified slightly the length of some links.

By comparing the six aspects such as direct kinematics, coupling degree, decoupling, reachable workspace, dexterous workspace and singularity, it is found that the comprehensive performance of the CRM is superior to that of 3-RRR typical manipulator.

5. Conclusions

Two disadvantages of the typical 3-RRR planar manipulator could be overcome by its topological structure optimization. It leads to the resulting kinematic performance are improved.

(1) The analytical solutions for the direct kinematics of the CRM can be obtained because of $k=0$. Its path planning, position control, and input-output motion decoupling properties are simpler.

(2) Based on the inverse kinematics, it can be obtained that the reachable workspace of the CRM is symmetric and continuous. Moreover, the dexterous workspace of it is bigger than typical mechanism's.

(3) Three kinds of singular configurations of this CRM are easier to be got. The singularity analysis of this mechanism is simpler than typical mechanism's.

In summary, the comprehensive kinematic performance of the coupling-reduced mechanism is superior. Structural decoupling-reducing is an effective approach for improving topological structure and its kinematic performances

Acknowledgements

This research is sponsored by the NSFC (Grant No. 51375062 and No.51475050), Jiangsu Key Development Project (No.BE2015043) and Jiangsu Scientific and Technology Transformation Fund Project (No. BA2015098).

References

- [1] Z. Huang, L. F. Kong and Y. F. Fang, "Theory and control of parallel robot mechanism," BeiJing: China Machine Press, 1997:1-34.
- [2] C. Gosselin and J. Merlet, "Direct kinematics of planar parallel manipulators: special architectures and number of solutions," Mechanism and Machine Theory, 1994: 1083-1097.
- [3] D. Oetomo, H.C. Liaw, G. Alici and B. Shirinzadeh, "Direct kinematics and analytical solution to 3-RRR parallel planar mechanisms," International Conference on Control, 2006:1-6.
- [4] C.M. Gosselin and J. Angeles, "The optimal kinematic design of a planar three-degree-of-freedom parallel manipulator, Journal of Mechanisms," Transmissions and Automation in Design, 1988, 110(3):35 -41.
- [5] J. Wu, J.S. Wang and Z. You, "A comparison study on the dynamics of planar 3-DOF 4-DOF,3-RRR and 2-RRR parallel manipulators," Robotics and Computer-Integrated Manufacturing, 2010, 2011, 27(1): 150-156.
- [6] S.-H. Cha, T.A. Lasky and S.A. Velinsky, "Determination of the kinematically redundant active prismatic joint variable ranges of a planar parallel mechanism for singularity-free trajectories," Mechanism and Machine Theory, 44(2009) 1032-1044.
- [7] X. Wei and J. Wu, "Dexterity of 3-RRR planar parallel manipulators," Machine tool and Hydraulics, 1001-3881 (2009) 10-051-3.
- [8] D.H. Li and S.T. Song, "Research of the reachable workspace of symmetrical planar 3-RRR parallel mechanism," Journal of Mechanical Transmission, 1004-2539(2015) 09-0029-03.
- [9] J.K. Cui, "On the dexterous workspace of 3-RRR planar parallel manipulator," University of Shanghai for Science and Technology, 1007-6735(2005)04-0365-04.
- [10] Z.H. Lan and M.W. Su, "Analysis of dextrous workspace and cavity of Planar Parallel Manipulator," Proceedings of the Twelfth National Institute of Institutional Studies, 2000.
- [11] F. Gao, X.J. Liu and X. Chen, "The relationships between the shapes of the workspaces and the link lengths of 3-DOF symmetrical planar parallel manipulators," Mechanism and Machine Theory, 36 (2001)205-220.
- [12] T. L. Yang, A.X. Liu and Y.F. Luo, "Theory and application of robot mechanism topology," Beijing: Science Press, 2012.
- [13] H.P. Shen, L.J. Yang, Q.M. Meng and H.B. Yin, "Topological structure coupling-reducing of parallel mechanisms," The14th IFToMM World Congress, Taipei, Taiwan, October 25-30, 2015.
- [14] C. Gosselin and J. Angeles, "Singularity analysis of closed-loop kinematic chain," IEEE International Conference on Robotics and Automation, Cincinnati: Computer Society Press, 1990, 6(3): 281-290.